Investigating the stability of frequency-dependent locally reacting surface boundary conditions in numerical acoustic models

Stephen Oxnard

Citation: The Journal of the Acoustical Society of America **143**, EL266 (2018); doi: 10.1121/1.5030917
View online: https://doi.org/10.1121/1.5030917
View Table of Contents: http://asa.scitation.org/toc/jas/143/4
Published by the Acoustical Society of America

Stephen Oxnard: JASA Express Letters https://doi.org/10.1121/1.5030917 Published Online 17 April 2018

Investigating the stability of frequency-dependent locally reacting surface boundary conditions in numerical acoustic models

Stephen Oxnard
Department of Computing and Technology, Anglia Ruskin University, East Road, Cambridge, CB1 1PT, United Kingdom
stephen.oxnard@anglia.ac.uk

Abstract: Numerical acoustic modeling enables simulation of sound propagation through bounded space. Recent research directed to refining Finite Difference Time Domain solutions for acoustic prediction has focused on emulating sound wave-surface interaction. Locally reacting surface properties are a popular choice for deriving boundary conditions that incorporate surface absorption properties. However, implementation of these boundary conditions, using the methods described in prevalent literature, is demonstrated here as unstable for complex room geometries. This work presents a reformulated implementation of frequency-dependent locally reacting surface boundary conditions for Finite Difference Time Domain simulations that is empirically demonstrated to be robust against simulation instabilities.

[CCC]
Date Received: January 8, 2018 **Date Accepted:** March 23, 2018

1. Introduction

Virtual room acoustic modeling is achieved by simulating sonic components (e.g., specular reflections, diffusion, and diffraction) that together comprise the system of enclosed sound propagation. To this end, numerical acoustic modeling techniques, such as Finite Difference Time Domain (FDTD) simulations (Botteldooren, 1995; Savioja *et al.*, 1994), yield solutions to the discrete wave equation. This wave-based approach preserves low frequency wave characteristics (such as diffraction and resonances) which are omitted when alternative geometric modeling techniques are used, e.g., ray tracing or the image-source method (Savioja and Svensson, 2015). Hence, FDTD simulations are pertinent to room acoustic modeling for low frequency sound propagation. Recent work on FDTD simulations has focused on the emulation of surface absorption characteristics (Bilbao and Hamilton, 2017; Kowalczyk, 2010). In particular, Locally Reacting Surface (LRS) boundary conditions (Kowalczyk and van Walstijn, 2008a; Kuttruff, 2009) govern wave-surface interaction in terms of material absorption characteristics and incident/reflected pressure wave amplitudes for localized surface regions and are, therefore, well-suited to FDTD simulations over discrete space.

However, the application of LRS conditions, as defined in Kowalczyk (2010) and Kowalczyk and van Walstijn (2008a), has been shown to give rise to numerical instabilities in FDTD simulations. This is demonstrated by Botts and Savioja (2014), who show that growing (unstable) solutions of the discrete wave equation are produced when implementing the LRS condition for non-cuboid spatial domains and high surface impedance values. Under these conditions, the numerical eigenvalue spectra may contain values above unity, thereby violating the numerical stability criterion for iterative wave equation solutions. To date, the analysis of such instability issues has been restricted to frequency-independent boundary conditions. This article provides an alternative formulation of the frequency-dependent LRS boundary condition defined in Kowalczyk (2010) and Kowalczyk and van Walstijn (2008b) based on "velocity-centered" FDTD approximations that are shown by Botts and Savioja (2014) to avoid unstable numerical solutions. Simulation results show that the original frequency-dependent LRS implementation becomes unstable for combinations of complex room models and high impedance boundaries, whereas the new formulation maintains numerical stability.

2. LRS implementation in FDTD acoustic models

The following discussion of LRS boundary conditions is presented here with reference to the iterative "leap-frog" FDTD solution to the wave equation for a target three-dimensional (3D) (in space) acoustic pressure field, after Kowalczyk and van Walstijn (2011):

$$p^{n+1}_{i,j,k} = \lambda^2(S^n_{i,j,k}) + 2(1-3\lambda^2)p^n_{i,j,k} - p^{n-1}_{i,j,k}, \tag{1}$$

where

$$S^n_{i,j,k} = p^n_{i+1,j,k} + p^n_{i-1,j,k} + p^n_{i,j+1,k} + p^n_{i,j-1,k} + p^n_{i,j,k+1} + p^n_{i,j,k-1}, \tag{2}$$

for pressure, p, using integers i, j, k, and n to describe the systems position in discrete 3D space (iX, jX, kX) with spatial sampling interval X (m) and discrete time, nT (s), with temporal sampling period $T = 1/F_s$ (s), where F_s is the temporal sampling rate (Hz). The Courant number, λ, relates these terms together with the wave speed, c (ms^{-1}), by $\lambda = cT/X$. Following Kuttruff (2009), the locally reacting surface condition is expressed as

$$\frac{\partial p}{\partial t} = -c\zeta_\omega \frac{\partial p}{\partial N}, \tag{3}$$

where ζ_ω is a frequency-dependent material impedance value for a surface with normal N (t and p are as previously defined). Kowalczyk and van Walstijn (2008b) were the first to formulate a frequency-dependent implementation of the LRS condition in FDTD models by digital filtering. In brief, this implementation initiates by expressing ζ_ω as a discrete transfer function in the z-domain, i.e., $\zeta_\omega = b_0 + B(z)/a_0 + A(z)$ where A and B are polynomials of z (Kowalczyk and van Walstijn, 2008b). The so-called "pressure-centered" (Botts and Savioja, 2014) approximation to LRS conditions in leap-frog FDTD simulations is achieved by applying first-order centered-difference approximations to Eq. (3) to solve for the pressure at nodes that lie outside the modeled domain [referred to as "ghost nodes" (Kowalczyk, 2010)]. For example, a right-hand surface boundary expression contains the ghost-node $p^n_{i+1,j,k}$ which may be expressed with a discretized form of Eq. (3) as

$$p^n_{i+1,j,k} = -\frac{1}{\lambda\zeta_\omega}\left(p^{n+1}_{i,j,k} - p^{n-1}_{i,j,k}\right) + p^n_{i-1,j,k}, \tag{4}$$

which, when substituted into Eq. (1) provides an appropriate absorbing update expression for boundary nodes on a right-hand surface. A more detailed description of this boundary formulation is provided in Kowalczyk (2010).

An alternative "velocity-centered" LRS implementation was originally investigated in terms of numerical stability by Botts and Savioja (2014) and was shown to mitigate unstable eigenvalue solutions. In contrast to the use of only centered-difference approximations to Eq. (3), a first-order backward- or forward-difference approximation is applied to the spatial derivative depending upon the orientation of the surface normal. For example, a right-hand surface boundary update expression is derived with a forward-difference approximation applied to the spatial derivative, yielding Eq. (5),

$$p^n_{i+1,j,k} = -\frac{1}{2\lambda\zeta_\omega}\left(p^{n+1}_{i,j,k} - p^{n-1}_{i,j,k}\right) + p^n_{i,j,k}. \tag{5}$$

Note that a left-hand surface boundary requires a backward-difference approximation to the spatial derivative of Eq. (3) to solve for the ghost node $p^n_{i-1,j,k}$. Direct substitution of Eq. (5) into the discrete wave equation, Eq. (1), provides a suitable update expression. First, the substitution of $p^n_{i+1,j,k}$ gives Eq. (6),

$$p^{n+1}_{i,j,k} = \lambda^2\left[-\frac{1}{2\lambda\zeta_\omega}\left(p^{n+1}_{i,j,k} - p^{n-1}_{i,j,k}\right) + p^n_{i,j,k} + p^n_{i-1,j,k} + p^n_{i,j+1,k} + p^n_{i,j-1,k} + p^n_{i,j,k+1} + p^n_{i,j,k-1}\right] + (2-6\lambda^2)p^n_{i,j,k} - p^{n-1}_{i,j,k}. \tag{6}$$

This expression can be rearranged into an explicit update expression for a right-hand surface boundary node, Eq. (7), considering $\zeta_\omega = b_0 + B(z)/a_0 + A(z)$ and defining $C(z) = \lambda A(z) + 2B(z)$, $D(z) = \lambda A(z) - 2B(z)$,

$$p^{n+1}_{i,j,k} = \frac{1}{\lambda a_0 + 2b_0}\Big(2\lambda^2(b_0 + B(z))\left(p^n_{i-1,j,k} + p^n_{i,j+1,k} + p^n_{i,j-1,k} + p^n_{i,j,k+1} + p^n_{i,j,k-1}\right) + 2(b_0 + B(z))(2-5\lambda^2)p^n_{i,j,k} + (\lambda a_0 - 2b_0 + D(z))p^{n-1}_{i,j,k} - C(z)p^{n+1}_{i,j,k}\Big). \tag{7}$$

Update expressions for edge and corner nodes are derived by successive substitution of undefined terms for ghost nodes that fall outside the modeled domain. Hence, for a right-hand rear edge, the same procedure is followed to solve for $p^n_{i+1,j,k}$ and $p^n_{i,j+1,k}$ leading to the update equation given in Eq. (8),

$$p^{n+1}_{i,j,k} = \frac{1}{\lambda a_0 + b_0}\Big(\lambda^2(b_0 + B(z))\big(p^n_{i-1,j,k} + p^n_{i,j-1,k} + p^n_{i,j,k+1} + p^n_{i,j,k-1}\big) + (b_0 + B(z))(2 - 4\lambda^2)p^n_{i,j,k} + (\lambda a_0 - b_0 + D(z))p^{n-1}_{i,j,k} - C(z)p^{n+1}_{i,j,k}\Big), \quad (8)$$

where $C(z) = \lambda A(z) + B(z)$, $D(z) = \lambda A(z) - B(z)$ and the frequency-dependent impedance ζ_ω is defined at the edge nodes themselves. Finally, for a top, right-hand rear corner the update expression is given in Eq. (9),

$$p^{n+1}_{i,j,k} = \frac{1}{3\lambda a_0 + 2b_0}\Big(2\lambda^2(b_0 + B(z))\big(p^n_{i-1,j,k} + p^n_{i,j-1,k} + p^n_{i,j,k-1}\big) + 2(b_0 + B(z))(2 - 3\lambda^2)p^n_{i,j,k} + (3\lambda a_0 - 2b_0 + D(z))p^{n-1}_{i,j,k} - C(z)p^{n+1}_{i,j,k}\Big), \quad (9)$$

where $C(z) = 3\lambda A(z) + 2B(z)$, $D(z) = 3\lambda A(z) - 2B(z)$ and the frequency-dependent impedance ζ_ω is defined at the corner nodes themselves. Expressions for all remaining orientations of boundary nodes on a cubic lattice can be calculated following this procedure.

3. Experimental procedure

LRS boundary conditions formulated for leap-frog FDTD schemes can be demonstrated to be stable when considering each boundary node condition in isolation. Numerical instabilities arise when the modeled domain is non-cuboid and/or contains combinations of "re-entrant" (non-convex) structures. However, the modeling of such structures is essential for arbitrary room acoustic simulation. For the purposes of this study, the wave equation is simulated using small cubic lattice topologies which incorporate different re-entrant (non-convex) edge and/or corner structures. Examples are depicted in Figs. 1(a)–1(f). The first two, domains (a) and (b) of size 11^3 voxels, were investigated by Botts and Savioja (2014) and shown to be unstable and stable when simulated with pressure-centered frequency-independent LRS boundaries, respectively. A further 120 voxelized test domains are defined by iteratively removing a random surface voxel from a 7^3 lattice domain, while maintaining an immutable 3^3 central voxel volume core, such that all remaining voxels represent air, surface, edge, or corner nodes. These domains represent a large, geometrically diverse range of non-convex structures and combinations thereof that could exist in a voxelized room acoustic model. Examples of such domains are given in Figs. 1(c)–1(f).

Each domain is simulated with both pressure- and velocity-centered Digital Impedance Filter (DIF) LRS boundary formulations for two different surface material filters. The first filter (DIF1) models the surface impedance properties of a highly reflective material, with ζ_{ω_1} varying between 200 and 400, while the second (DIF2) maintains a higher impedance value, ζ_{ω_2}, varying between 500 and 1000. These impedance values impose similar conditions to those applied by Botts and Savioja (2014) when testing for numerical instability and are defined for all frequencies up to the Nyquist frequency (in this case $F_s/2 = 14.2$ kHz in order to produce reasonable simulation run-times). The wave speed is set at $c = 344$ ms^{-1} and the inter-nodal grid spacing set to the Courant limit $X = \sqrt{3}cT$ m for numerical stability [see Kowalczyk (2010)]. The input excitation signal is the Kronecker delta function with a direct current removal filter applied. The excitation and receiver locations are defined to be the center voxel in all domains. MATLAB simulation scripts, filter coefficients [calculated using the MATLAB filter design function (Mathworks (2018), MathWorks Inc., Natick, MA)], and domain definitions used to render results are available online for reference (Oxnard, 2018).

An empirical experiment was conducted to test the hypothesis that previously presented velocity-centered FDTD formulation of frequency-dependent LRS boundaries are robust against numerical instability for modeled non-cuboid domains with non-convex structures, while pressure-centered formulations of the same conditions are not. Results obtained are in support of this hypothesis. These results are drawn from analysis of 488 rendered Room Impulse Responses (RIRs) that correspond to the 122 domain topologies, two DIF-based LRS boundary formulations, and two DIF definitions previously described.

4. Results and discussion

Simulated RIRs for domains (a)–(f) and filters DIF1 and DIF2, using both pressure-centered (P) and velocity-centered (V) LRS boundary implementations, are displayed in Fig. 1. In domain (a), the pressure-centered boundary implementation produces a numerically unstable system for both impedance filter definitions. This is demonstrated by the absolute amplitude envelopes of the RIRs P-DIF1 and P-DIF2 which tend to infinity. In domain (b), the pressure-centered approach yields a stable simulation. These results, which are in agreement with those presented by Botts and Savioja

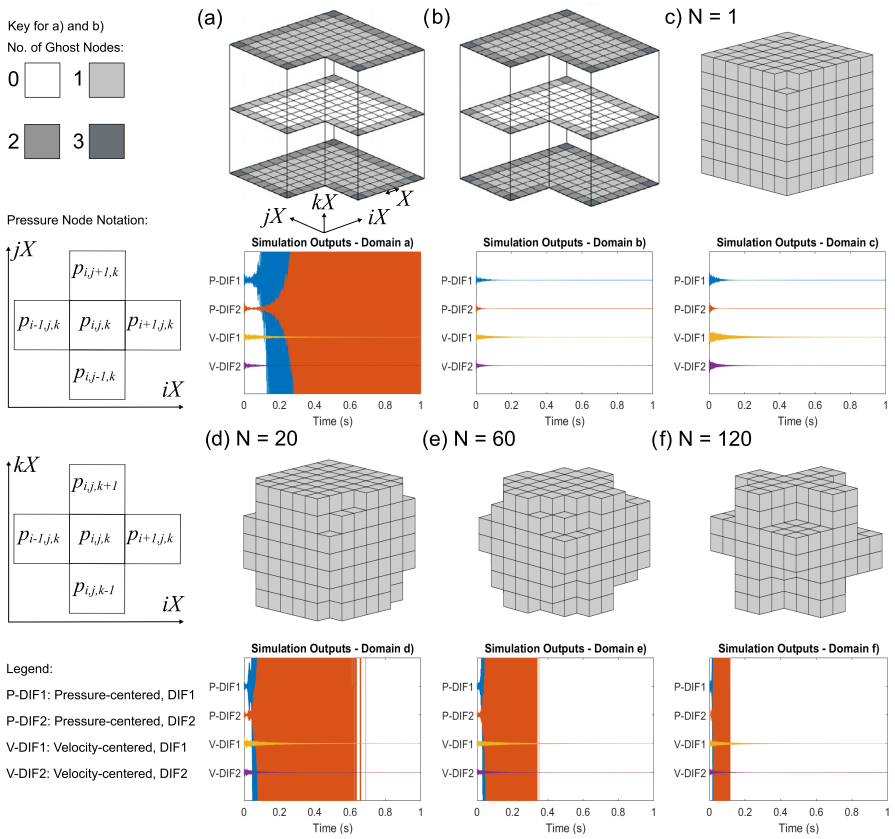

Fig. 1. (Color online) Examples of simulated domains (a)–(f). Diagrams for domains (a) and (b) are adapted from Botts and Savioja (2014) along with the neighbouring node key shown to the left of domain (a). The node and axis notation is given below. Domains (c)–(f), produced by the iterative algorithm described earlier, incorporate non-convex structures by removal of N voxels from a 7^3 voxel domain. RIRs rendered for each domain are displayed below the corresponding domain diagram.

(2014), serve to highlight the conditional stability provided by pressure-centered LRS boundary formulations. In contrast, domains (a) and (b) are successfully rendered using the velocity-centered formulation, derived in Sec. 2, which provides stable RIR simulation for both impedance filters (these are denoted V-DIF1 and V-DIF2). The difference in decay characteristics observed between the stable velocity- and pressure-centered implementations is a consequence of the different finite difference approximations used to model the boundary conditions [see Hamilton (2016) for rigorous analysis of these properties]. The simulation of domains (c)–(f) further demonstrates the conditional stability of the pressure-centered boundary formulation. As shown in Fig. 1, pressure-centered conditions give rise to numerical instability in complex domain topologies, (d)–(f), for P-DIF1 and P-DIF2. Of the 120 domains, defined using the iterative voxel removal process, the pressure-centered boundary formulation simulations maintained stability for 3 cases ($N < 4$) for P-DIF1 and 7 cases ($N < 8$) for P-DIF2 corresponding to a success rate of 0.042%. The use of the velocity-centered formulation provides stable simulations for all 120 test domains with both filters achieving a 100% success rate. Overall, this experiment further exposes the conditional stability of pressure-centered LRS boundaries when applied to non-cuboid domains with non-convex structures. The velocity-centered approach, formulated in this work, is shown to provided consistently stable simulations for all modeled domains.

5. Conclusion

A refined approach to frequency-dependent LRS boundary condition implementations in FDTD numerical acoustic models has been presented and examined in terms of numerical stability. Objective data rendered through simulation of a series of RIRs for increasingly complex discretized target acoustic fields supports the claim that velocity-centered formulations of frequency-dependent boundary conditions are robust against numerical instability and prominent alternative pressure-centered approaches (Kowalczyk, 2010; Kowalczyk and van Walstijn, 2008a,b) are not. Hence, it has been demonstrated that velocity-centered implementations of frequency-dependent boundary

conditions may be used to perform numerically stable FDTD acoustic simulations of complex room geometries for the purpose of acoustic analysis and prediction.

References and links

Bilbao, S., and Hamilton, B. (**2017**). "Wave-based room acoustics simulation: Explicit/implicit finite volume modeling of viscothermal losses and frequency-dependent boundaries," J. Audio Eng. Soc. **65**(1–2), 78–89.

Botteldooren, D. (**1995**). "Finite-difference time-domain simulation of low-frequency room acoustic problems," J. Acoust. Soc. Am. **98**(6), 3302–3308.

Botts, J., and Savioja, L. (**2014**). "Spectral and pseudospectral properties of finite difference models used in audio and room acoustics," IEEE/ACM Trans. Audio, Speech Lang. Process. **22**(9), 1403–1412.

Hamilton, B. (**2016**). "Finite difference and finite volume methods for wave-based modelling of room acoustics," Ph.D. dissertation, University of Edinburgh, Edinburgh, UK.

Kowalczyk, K. (**2010**). "Boundary and medium modelling using compact finite difference schemes in simulations of room acoustics for audio and architectural design applications," Ph.D. dissertation, Queen's University, Belfast, Ireland.

Kowalczyk, K., and van Walstijn, M. (**2008a**). "Formulation of locally reacting surfaces in FDTD/K-DWM modelling of acoustic spaces," Acta Acust. united Acust. **94**(6), 891–906.

Kowalczyk, K., and van Walstijn, M. (**2008b**). "Modeling frequency-dependent boundaries as digital impedance filters in FDTD and K-DWM room acoustics simulations," J. Audio Eng. Soc. **56**(7/8), 569–583.

Kowalczyk, K., and van Walstijn, M. (**2011**). "Room acoustics simulation using 3-D compact explicit FDTD schemes," IEEE Trans. Audio, Speech Lang. Process. **19**(1), 34–46.

Kuttruff, H. (**2009**). *Room Acoustics*, 5th ed. (Taylor & Francis, London).

MathWorks Inc. (**2018**). "Filter design using MATLAB," available at https://uk.mathworks.com/discovery/filter-design.html (Last viewed March 15, 2018).

Oxnard, S. (**2018**). "Stability of locally reacting surface boundary conditions in fdtd acoustic simulations," Open Science Framework online asset repository, available at https://osf.io/7ukcx/ (Last viewed March 15, 2018).

Savioja, L., Rinne, T. J., and Takala, T. (**1994**). "Simulation of room acoustics with a 3-d finite difference mesh," in *Proceedings of International Computer Music Conference*, Aarhus, Denmark, pp. 463–466.

Savioja, L., and Svensson, U. P. (**2015**). "Overview of geometric room acoustic modelling techniques," J. Acoust. Soc. Am. **138**(2), 708–730.